Charging Mitigation Strategies in Imaging Insulating Polymer Spheres via Low Voltage Field Emission Scanning Electron Microscopy

Application Note

Jining Xie
Agilent Technologies

Introduction

Because of its high resolution, broad range of magnifications and straightforward image interpretation, scanning electron microscopy (SEM) is one of the common imaging techniques for morphological characterization of polymeric materials with various shapes, crystalline forms, and dimensions. Unfortunately, there are some technical difficulties that make SEM study of polymers quite challenging. The most notorious impediment of polymer imaging by SEM is charging because most polymers are highly insulating (volume resistivity $\cong 10^{15}$–$10^{20}\Omega\cdot$cm). When the primary electron beam impinges on a polymer specimen, the localized excess electrons cannot be conducted away giving rise to a negative charge accumulation which may cause annoying artifacts such as abnormal contrast, image distortion and shift. Coating the insulating polymer specimen with a metallic thin film is normally implemented to overcome the charging problems. However, the intrinsic nanostructure of the coating might be discernable at high magnifications unless special metals (e.g. Cr, Ir) are selected with meticulous deposition procedures. Furthermore, the thin metal coating might obscure the fine surface details of polymer materials under investigation. Another option is to image insulating polymers in a low vacuum mode where gas in the specimen chamber can absorb some excess electrons. Generally, this imaging mode gives an inferior spatial resolution. Another dilemma in SEM imaging of polymers is the low contrast. Polymers usually consist of light elements (C, H, O and others). The low atomic numbers of these elements in conjunction with the low density of polymer results in a weak interaction between the specimen atoms and the incident electrons leading to a poor contrast [1, 2]. Possible methods to enhance such a poor compositional contrast are heavy-atom staining and chemical extraction. In addition, polymers are susceptible to beam-induced radiation damages. Since most of the energy carried by the electron beam would convert to heat, the stability of polymer specimen when exposed to the beam is by all means an issue to be concerned. Deterioration, decomposition, sublimation, and evolution of gases/molecules may occur during SEM imaging resulting in morphological deformation and/or dimensional changes of polymers.

The resurgence in interest in the low voltage scanning electron microscopy (LV-SEM) can be attributed to those recently improved technologies in modern SEMs including high-brightness field emission gun (FEG), precise electron optics, and well-control engineering tolerance, etc. For morphological imaging of polymeric materials, low voltage field emission SEM (LV-FESEM) is highly promising due to its high spatial resolution, enhanced image contrast, reduced/localized beam damage, and possible elimination of metal coating. The

purpose of this note is to study the charging phenomenon in low voltage imaging and demonstrate some practical approaches on an Agilent 8500 compact LV-FESEM for charging control in imaging uncoated polystyrene spheres.

Low Voltage Imaging for Polymers

LV-SEM is generally referred to as a SEM that has a primary electron beam with landing energy of less than 5 keV. In order to better understand the advantages of LV-SEM in imaging polymers, it is necessary to discuss some unique features associated with signal formation and detection at low voltages. During SEM imaging, a highly focused electron beam scans the surface of the specimen, pixel by pixel, and the beam/specimen interaction generates secondary electrons (SE) and backscattered electrons (BSE) followed by detection of their escaped portions. By taking the customary notations: SE yield δ (number of emitted SEs per incident electron), BSE yield η (number of emitted BSEs per incident electron) and total yield σ (total number of emitted electrons per incident electron), the Kirchhoff's law can be expressed as:

$$I_{BC} = \delta I_{BC} + \eta I_{BC} + I_{SC} \quad (1)$$

$$I_{BC} = \sigma I_{BC} + I_{SC} \quad (2)$$

where I_{BC} is the beam current, and I_{SC} is the specimen current flowing to or from ground. At the situation of scanning the specimen surface with a beam energy higher than 5 keV, σ is less than unity, and excess charges will deposit on the surface. It is not a problem for conductive materials since these excess charges can be conducted away

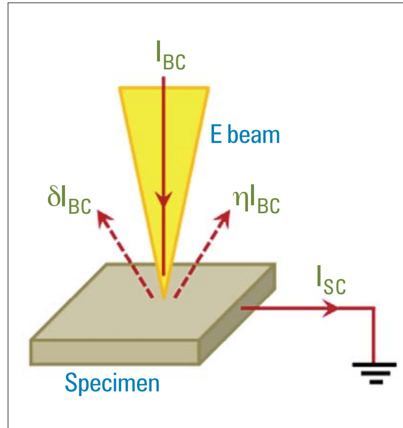

Figure 1. Schematic of currents on the specimen during scanning by an incident electron beam.

to ground maintaining the specimen in the neutral condition, as illustrated in Figure 1. However, for insulating polymeric materials, I_{SC} equals to zero, thereby charges will build up on the surface acquiring a negative potential. As a consequence, this negative potential may induce the deflection of the incident beam, repelling of emitted SEs, periodic bursts of SEs and strikingly increase the SE emission at the edges which result in anomalous contrast and brightness.

Interestingly, it was found that the total yield σ can be larger than unity at low beam voltages. Attempts have been made to not only formulate a theory to predict a yield curve but also verify it by experimental measurements [3]. In view of the fact that η is typically 10 times less than δ, it is reasonable to ignore the direct contribution of BSEs to the total emission current for simplification purpose in theory prediction. The relationship between the SE yield δ and the beam voltage E can be expressed as:

$$\left(\frac{\delta}{\delta_{max}}\right) = 1.11 \left(\frac{E}{E_{max}}\right)^{-0.35} \left\{1 - \exp\left[-2.3\left(\frac{E}{E_{max}}\right)^{1.35}\right]\right\} \quad (3)$$

where δ_{max} is the maximum SE yield at the beam energy E_{max} [4]. Figure 2a depicts a "universal" yield curve for SE emission showing its characteristic parameters: maximum SE yield δ_{max} at the beam voltage E_{max} and the "cross-over" points, E_1 and E_2. Compared with conducting materials, polymers' yield curves have different shapes with a much sharper maximum at small values and then decrease more rapidly [5]. It can be seen that the SE yield rises when the incident beam energy drops from high energies (>10 keV). When the incident beam energy is further reduced to a value lower than E_2, the SE yield is larger than unity. At this situation, negative charging will convert to positive charging on the insulating specimen. The SE yield reaches its maximum value δ_{max} at the beam energy E_{max}. After that the SE yield drops with the beam energy. These two "cross-over" points E_1 and E_2 represent two "perfect" neutral charging conditions for SEM imaging where the number of incident electrons equals to that of emitted electrons. Since the E_1 values for most materials are too low for SEM operation (<200 eV), the E_2 values must be the most important parameter for insulating materials in LV-SEM imaging.

Extensive research efforts have been made to establish the relationship between the SE yield and the physical/chemical properties of polymers [6]. One semi-empirical model of SE yield for polymers has been proposed by fitting

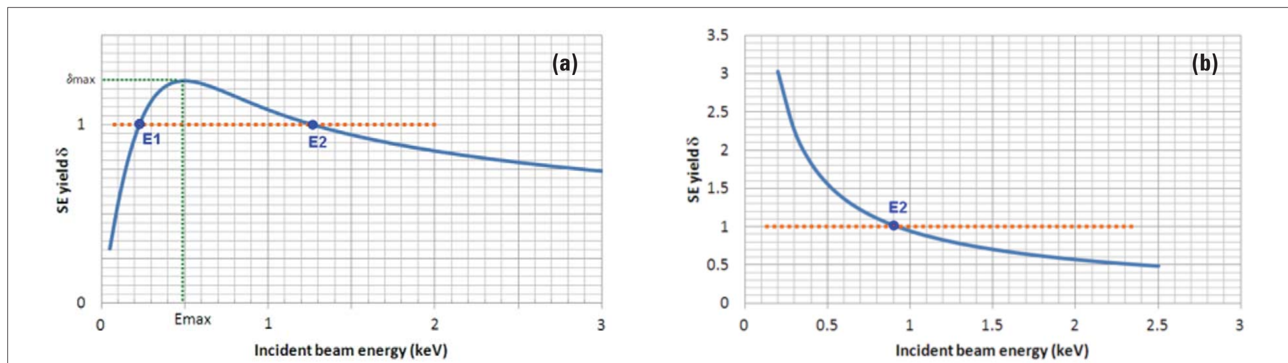

Figure 2. (a) Plot of the "Universal" SE yield curve; (b) plot of calculated SE yield of polystyrene vs. the incident beam energy.

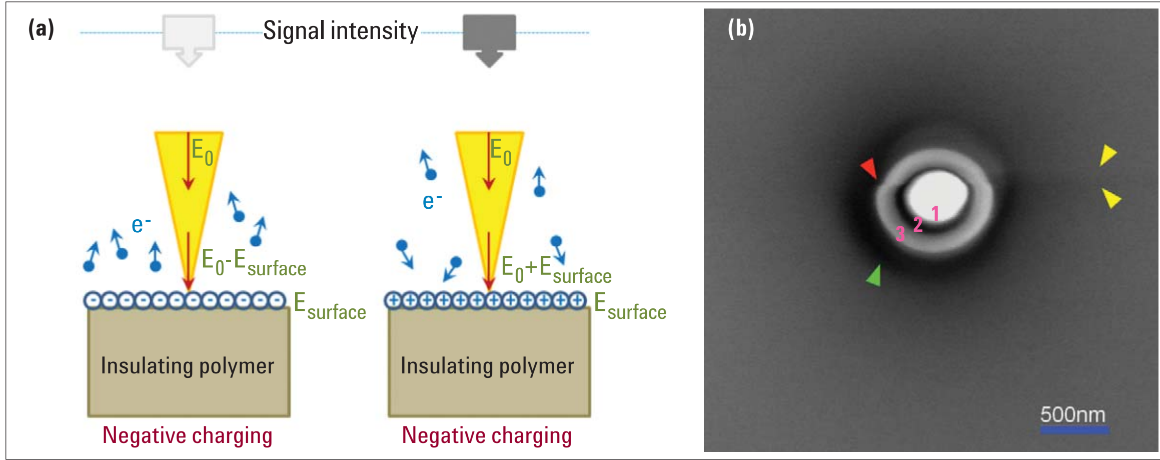

Figure 3. (a) Schematic depicting the effects of negative and positive charging conditions on SE signal detection; (b) a typical SE image of an individual polystyrene bead on Si showing several charging effects.

measured results to the "universal yield" equation **(3)** as:

$$\delta = \left[10.64\left(\frac{VE}{MW}\right) - 3.15\right]E^{-0.725} \quad (4)$$

where VE and MW are the number of valence electrons and molecular weight per monomeric unit, respectively. Equation **(4)** clearly implies that the quantity (VE/MW) is a significant index for SE yields of polymers. Also, the E_2 value can be calculated by setting δ as unity. For polystyrene, VE=40 and MW=104, then its SE yield formula changes to:

$$\delta_{polystyrene} = 0.9423E^{-0.725} \quad (5)$$

The SE yield curve for polystyrene is plotted in Figure 2b, and the E_2 value is around 0.92 keV. An improved approach was developed by incorporating the simple electron diffusion model, as described above, in a Monte Carlo trajectory simulation of electron scattering [7]. Calculated SE and BSE yields by using this model are in excellent agreement with measurement results. It is noteworthy to point out here that, other than the composition and molecular bonds, the SE yield of polymers can be determined by a variety of physical parameters such as crystalline nature, density, and surface roughness, etc. Likewise, the predicted E_2 values for certain polymeric materials, to some extent, can only provide a useful guidance towards a proper selection of the beam voltage for imaging.

Higher contrasts are expected for LV-SEM probably due to several reasons. First, the higher SE yield at low beam voltages suggests more signal per incident electron. Maximum topographic contrast can be achieved when the SE yield is maximized. Secondly, the significantly reduced electron range at low voltages means a more localized beam/specimen interaction resulting in an enhanced contrast. For instance, only the "real" edges display bright at low voltages. Thirdly, for LV-SEM, the combination of SE1, generated by the incident electrons, and SE2, produced by BSEs, contributes to a higher signal magnitude without sacrifice of resolution. When working at high beam voltages, the SE1 and SE2 signals come from ranges of a few nanometers and hundreds of nanometers, respectively, from the incident point. Therefore, the high resolution information is only carried by the SE1 signal, which has roughly 20-30% of the total SE signal intensity. At low voltages, because of the reduced interaction volume, both SE1 and SE2 carry high resolution contrast details.

Although less surface deformation was observed, it is still unknown whether or not working at low beam voltages induces less irradiation damage for polymers. Because of a smaller total electron deposition on a markedly reduced interaction volume at low voltages, the deposited energy density still can be substantially high which might cause irradiation damages locally. Hence the minimum-dose strategy for imaging will be very useful to obtain images with sufficient information in an acceptable quality.

Charging of Polystyrene Beads at Low Voltages

Since most of polymers have E_2 values ranging from 0.5 to ~3.0 keV, both negative and positive charging can be observed when imaging at low beam voltages. When incident electrons with energy $E_0 > E_2$ impinge the surface of polymer, excess charges will build up a negative potential $E_{surface}$. Such a negative potential can affect the SE detection in several ways such as repelling the emitted SEs from the surface, reducing the landing energy to E-$E_{surface}$, and increasing the potential difference between the detector and the polymer surface [8]. All of these effects actually enhance the detected SE signal with a bright appearance in the SE image. On the other hand, the positively charged area will appear dark in the SE image because of the attraction of emitted SEs to the surface. The influence of surface potentials on SE signal detection is illustrated in Figure 3a.

A typical SE image of an individual polystyrene bead (~850 nm in diameter) on a Si substrate reveals several features of the charging phenomenon, as shown in Figure 3b. This image was recorded at a beam voltage of 1 keV. An obvious scan discontinuity can be observed, as indicated by the red arrow head. This "tear" scan is usually a sign

of actual beam displacement caused by charging during scanning. There is a charging halo, appearing as a dark "ring", around the polystyrene bead on the Si substrate, pointed by the green arrow head. This halo phenomenon can be explained as the depressed SE detection in the vicinity of the polystyrene bead. The silicon substrate is semiconducting hence it can be always imagined as grounded. When the negative charging was established on the insulating polystyrene surface, the potential difference between polystyrene and silicon will create an electric field which may re-collect a large portion of emitted SEs to the Si substrate. Another discernable feature is a weak, black stripe (indicated by two yellow arrow heads), horizontally crossing the polystyrene bead. This charging artifact could be associated with amplifier saturation effects. On the polystyrene bead itself, three distinct areas, labeled as **1**, **2** and **3**, with different grey levels are evident. Apparently, area **1** can be assigned as a negatively charged area. Its extreme brightness completely obscures all surface details in that area. Contrarily, area **3** does not show any obvious charging effect, thereby can be attributed to a positively charged area. The reason for different areas in the same polystyrene beads exhibiting various charging statuses is the change of SE yield by the incident beam angles, which will be discussed in detail later. In regard to the dark "ring", area **2**, the mechanism of depressed SE signals could apply. In Agilent 8500, a microchannel plate (MCP) detector is used for both SE and BSE detections. A positive potential is applied on the MCP detector in the SE imaging mode, and it produces a field of ~200 V/cm attracting emitted electrons. Assuming a potential difference of only tens of volts is developed between area **1** and area **3** under the electron beam, the local field can be significantly stronger than that generated by the MCP detector. Consequently, emitted SEs may be attracted back to the surface, lowering the detected signal and displaying as the dark area **2**.

Note that polystyrene beads used in this study are all in sphere shapes with smooth surfaces. The harsh white-dark contrast due to the charging effect makes it almost impossible to recognize the real morphology of polystyrene beads. So it is desirable to look for a "stable" condition in which artifact-free images can be obtained.

Effects on Charging at Low Voltages

To study those factors that may influence the charging in LV-FESEM, a variety of imaging parameters/conditions were tested on polystyrene spheres on Si substrates [9]. For comparison purposes, only one variable was adjusted while others were kept identical in every test.

1. Effect of the beam voltage

Adjusting the beam voltage can be the first and the most effective approach to overcome charging when imaging insulating polymers. As discussed above, a polymer normally shows a great propensity to accumulate negative charges when scanned by an electron beam at energy higher than its E_2. Lowering the beam voltage is able to increase the SE yield and hence it is possible to convert the negative charging status to a positive one on the polymer surface. Compared with negative charging, positive charging is far more stable for image acquisition because of the so-called self-regulating process occurring at low voltages. A small positive potential can be neutralized, to a certain extent, by either re-collection of emitted SEs or electron evolvement from the specimen surface

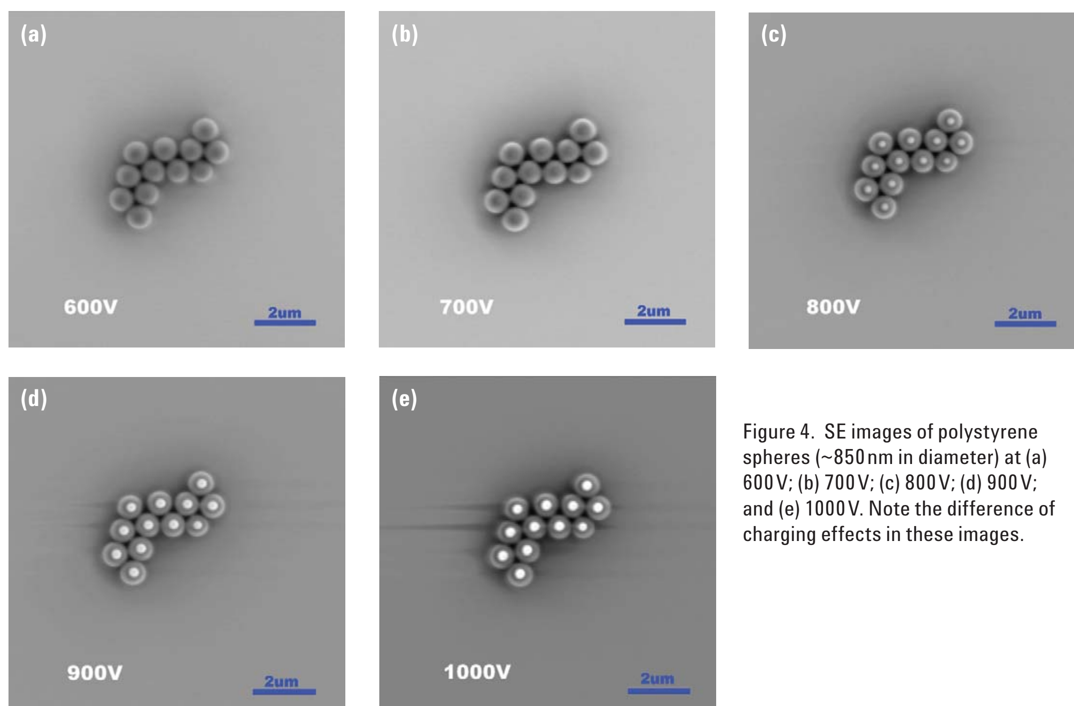

Figure 4. SE images of polystyrene spheres (~850 nm in diameter) at (a) 600 V; (b) 700 V; (c) 800 V; (d) 900 V; and (e) 1000 V. Note the difference of charging effects in these images.

so as to prevent the surface positive potential not higher than a few hundred millivolts [10].

In order to avoid any unnecessary charge build-up on a specimen surface which may be irreversible, imaging an insulating sample normally should start from the lowest beam energy workable in the instrument. Then it is hoped to observe the switching from positive charging to negative charging as the beam voltage is slowly increased. Generally, imaging with a low energy beam results in a worse resolution than in the case of a higher energy beam. This is primarily because of the lower gun brightness, larger wavelength, more severe lens aberration (especially chromatic aberration), and higher sensitivity to external interferences at a lower beam energy. Therefore, especially at the range of low voltages, a proper image with an adequate resolution and a sufficiently high signal-to-noise ratio needs to be recorded at the highest beam voltage not generating obvious negative charging effects. The beam voltage of an Agilent 8500 LV-FESEM can be adjusted continuously from 500 V to 2000 V due to its all-electrostatic lens design. It is convenient for users to achieve high quality images on insulating polymeric materials by a fine tuning of the incident beam energy.

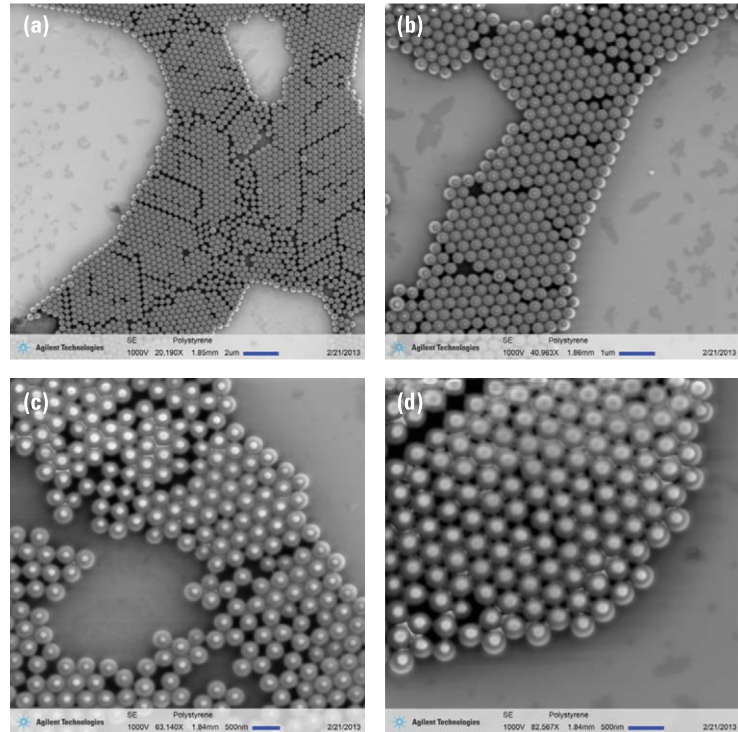

Figure 5. SE images of polystyrene beads (~400 nm in diameter) recorded at different magnifications: (a) ~20 kX; (b) ~40 kX; (c) ~60 kX and (d) ~80 kX. (The magnification values are displayed based on the 2048 x 2048 scanning resolution.)

Images in Figure 4 show the effect of the beam voltage on charging for polystyrene beads with an average diameter of ~850 nm. As expected, the image of 600 V, Figure 4a, clearly manifests a positive charging condition on the spheres. On each bead, the center area is identically in dark color, suggestive of a depressed SE emission. The image of 700 V, Figure 4b, displays almost the same features as those in Figure 4a. The exception is that a tiny bright spot can be barely seen in the center of each bead which can be regarded as an emergence of the negative charging. These bright spots are much more obvious in Figure 4c, an image recorded at 800 V. Not surprisingly, the center areas of beads become brighter and brighter as the beam voltage was raised to 900 V and 1000 V, as shown in Figure 4d and 4e, respectively. Additionally, the saturation effect-related black stripes are obvious at these conditions. Here, it is reasonable to associate the level of negative charging with the size of the bright area on the beads as well as the degree of anomalous contrast. And this will be used as a plausible criterion to qualitatively evaluate the magnitude of negative charging on polystyrene beads in this study. The E_2 value of bulk polystyrene was reported as 0.9–1.3 keV by both theoretical calculation and experimental measurement. For this particular polystyrene sample, slightly less than 700 V of E_2 can be estimated under the imaging condition.

2. Magnification effect

The charging effect is also a function of imaging magnifications in SEM. In practice, reducing the magnification is a common approach indeed to overcome any possible image distortion and harsh contrast related to the charging. Changing the magnification is actually achieved by varying the scan size on the specimen. Assuming the same beam current is used for scanning, a higher current density is the result of a smaller scan size. Experimental measurements suggest that the surface potential is closely related to the beam dose, and the effect is evident when working at a beam with its energy close to the E_2 value of the specimen [8]. Thus lowering magnification results in a decreased surface potential and a minimized dynamic charging, and thereby creates less charging effects.

This trend can be easily demonstrated on polystyrene beads with an average diameter of ~400 nm. All images shown in Figure 5 were recorded at 1000 V and the magnifications are labeled based on the 2048 x 2048 scanning resolution. Figure 5a at ~20 kX magnification clearly resolves the semi-regularly arranged polystyrene beads without any charging phenomenon. When the image magnification is increased to ~40 kX, small bright spots were observed on all beads, indicating a small negative potential development on the surface (Figure 5b). The charging problem is worse when imaging at ~60 kX. As can be seen from Figure 5c, the observed harsh contrast makes it difficult to interpret the image. As the magnification is further increased to ~80 kX, it is almost impossible to obtain a stable image in an acceptable quality.

Instead abnormal streaks can be seen, as shown on the top of Figure 5d. As a rule of thumb, the imaging magnification should be kept as low as is capable of achieving the needed pixel resolution to resolve the feature of interests on insulating specimens.

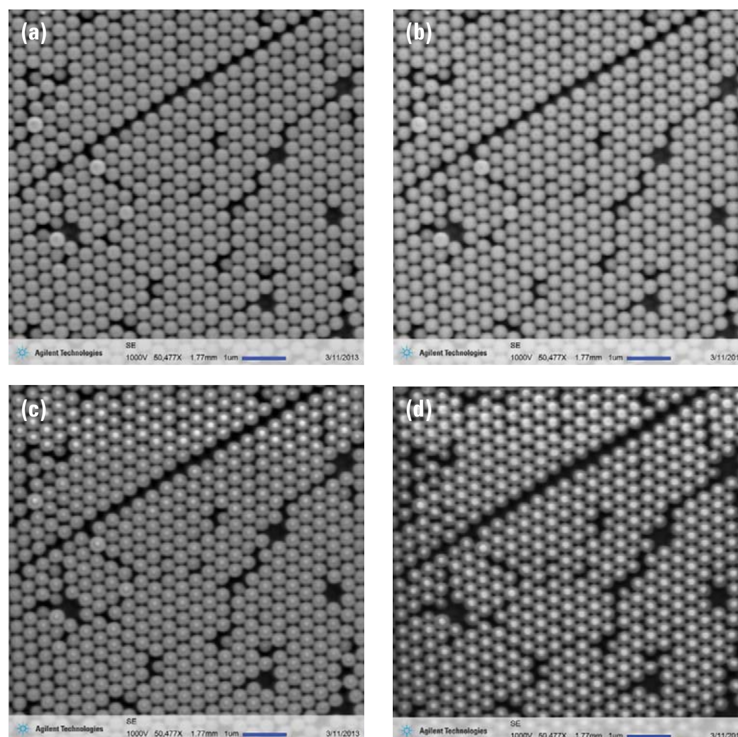

Figure 6. SE images of polystyrene spheres (~400 nm in diameter) recorded at different scanning rates. (a) dwelling time: 3.2 µs/pixel; (b) dwelling time: 6.4 µs/pixel; (c) dwelling time: 12.8 µs/pixel; (d) dwelling time: 25.6 µs/pixel.

3. Effect of the scanning rate

As another defence against sample charging, adjustment of the scanning rate is realized by varying the dwelling time on each pixel during beam rastering. For non-conductive samples, charging is time dependent. It has been well documented that fast scanning in SEM does not reduce charging, and it only stabilizes the charge distribution [11]. For insulating polymers, a specimen acts as a capacitor that undergoes charge-up and discharge processes on the surface alternatively during imaging. The charge-up process occurs when the beam impinges at a pixel with charge build up as a function of the dwelling time. The discharge process happens as the decay of accumulated charges when the beam moves away. The process of a full charge-up to its maximum surface potential is very fast (in the order of microseconds to nanoseconds), whereas the discharge one is much slower. In a fast scanning, the electron beam returns to the previously stroke pixel before the discharge process completes. This is a preferred condition for imaging acquisition because of the uniform charge distribution all over the imaging area.

Four different scanning rates were tested for imaging the same area of polystyrene spheres. Figure 6a, 6b, 6c and 6d are images obtained at dwelling times of 3.2 µs/pixel, 6.4 µs/pixel, 12.8 µs/pixel and 25.6 µs/pixel, respectively. Figure 6a does not show any charging effect, and it is believed that the uniform charge distribution prevents any possible electrostatic fields over the imaging area. This fast scanning rate is sufficient to produce stable images in a good quality. Similarly, charging effects are almost absent in Figure 6b, suggesting that the beads still float at a fairly stable potential at such a relatively slower scanning rate. This steady situation does not exist when the dwelling time is further increased. Both Figure 6c and 6d display evident charging on polystyrene beads, and they are certainly not adequate for morphological characterization.

4. Differences in scans in order

Similarly, the observed quality decline with scans in order can be explained by the dynamic charging. A comparison of three successive scans in an identical imaging condition on polystyrene beads is shown in Figure 7. The first scan produces an almost charging-free image showing the detailed surface

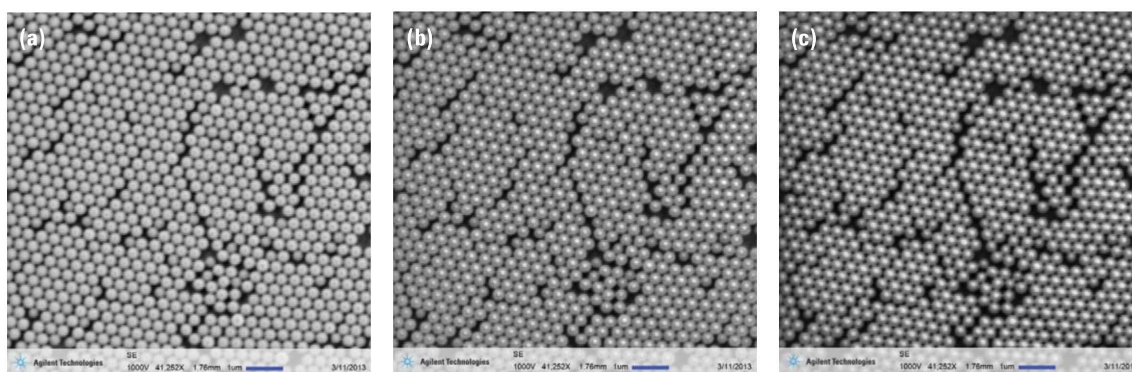

Figure 7. SE images of polystyrene beads recorded in order: (a) the 1st scan; (b) the 2nd scan; (c) the 3rd scan.

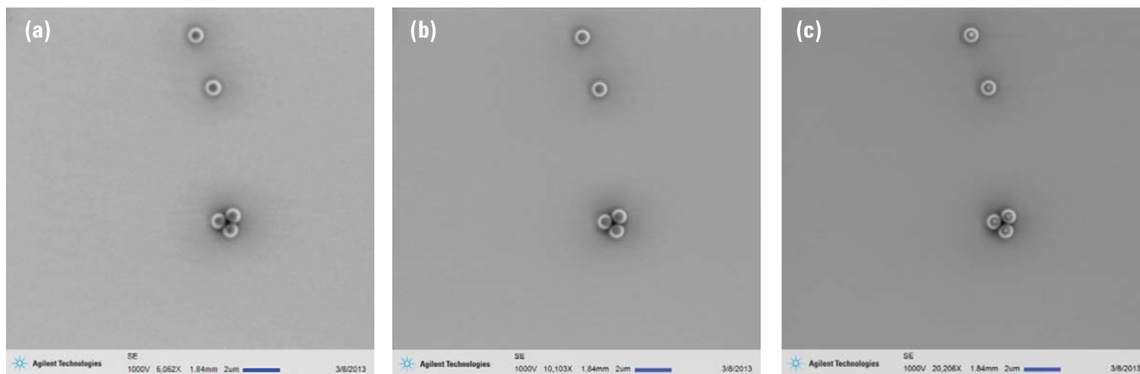

Figure 8. SE images of polystyrene beads recorded in various scanning resolutions: (a) 512 x 512; (b) 1024 x 1024; (c) 2048 x 2048.

morphology (Figure 7a). The adverse charging effect appears in the second scan, Figure 7b, and becomes even worse in the third scan, Figure 7c. It is likely that, even though negative charges started to accumulate from the beginning of beam scanning on the fresh surface, the negative potential still can be restrained within a relatively low level. And a uniform distribution of charges makes the first scan stable enough for image acquisition. During the following scans, the negative potential on the bead surface rose up to a certain level so that it can significantly affect both incident electrons and emitted SEs. This is quite a common problem in SEM imaging of insulating materials. A simple but always effective approach is to do focusing and stigmation correction on an area and then deflect the electron beam to an unexposed area nearby for imaging recording. Scanning the fresh surface on insulating polymers, with few exceptions, is more likely to obtain a satisfying image.

5. Effect of the scanning resolution

Agilent 8500 compact LV-FESEM has three scanning resolutions: 512 x 512, 1024 x 1024 and 2048 x 2048. It was observed that the charging phenomenon changes with the scanning resolution which can be explained by a combination of the dose effect on surface potential and charge distribution effect during scanning. Figure 8 compares images recorded at three scanning resolutions (at an identical scanning rate). Different from the magnification effect discussed previously, the same specimen area was scanned in all cases. The scanning resolution basically corresponds to the pixel resolution in the final image. Scanning the same area on the specimen but displaying with different pixel resolutions naturally gives rise to different pixel dimensions. The pixel dimensions of Figure 8a (in 512 x 512), 8b (in 1024 x 1024) and 8c (in 2048 x 2048) are calculated as 40 nm/pixel, 20 nm/pixel and 10 nm/pixel, respectively. Because of the same dwelling time in all cases, the electron dose of 2048 x 2048 is 4 times of that in 1024 x 1024 and 16 times of that in 512 x 512 on the same scanning area. A higher electron dose could results in a higher surface potential accompanying with a more severe charging. Meanwhile, similar mechanism to the scanning rate effect also applies here. The 512 x 512 scan requires the least time to finish one frame acquisition, and thereby it has the largest possibility to maintain the most uniform charge distribution resulting in the most stable image.

6. Averaging function for noise reduction

So far, we have seen that the strategy of fast scans at low scanning resolutions works well for imaging insulating polymers towards stable images. However, this approach inevitably reduces the signal-to-noise ratio. Thanks to the digital imaging acquisition and display technologies which are now commonly used in modern SEMs, the "averaging" function provides an effective way to improve

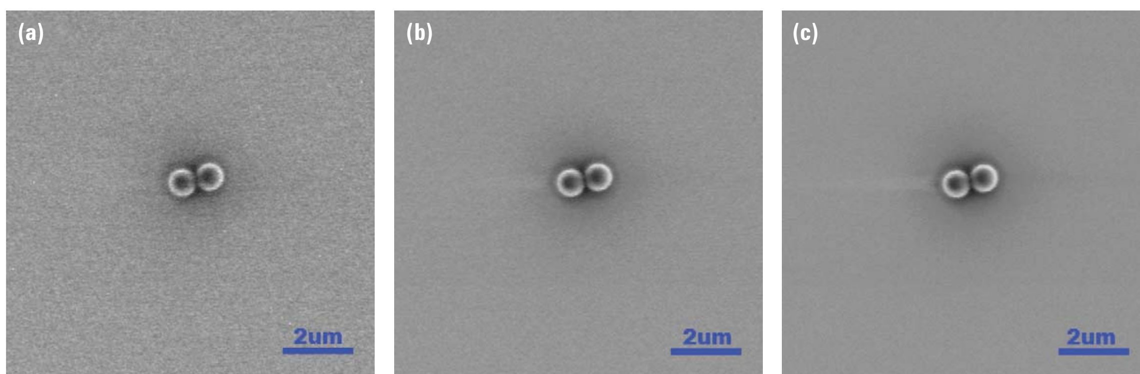

Figure 9. SE images of polystyrene spheres recorded at the 512x512 scanning resolution and a 6.4μs/pixel dwelling time. (a) The single frame image; (b) an image after 6 frame-averaging; (c) an image after 20 frame-averaging.

the image quality. For instance, the image shown in Figure 9a was recorded at the 512 x 512 scanning resolution with a 6.4 µs/pixel dwelling time. Under this condition, the charging effect is absent in the image. As expected, high level background noises can be seen which sometimes makes it difficult to resolve fine features. A digital image is composed of a number of pixels with different grey levels (e.g. 256 discrete levels for 8 bit digitization), which correspond to different signal intensities of detected electrons in SEM. The easy and powerful processing capability is regarded as one of the prime advantages for digital images. Averaging several frames not only cancels those random noises, but also enhances the "true" signals coming from the real morphology. The software of Agilent 8500 provides such a "frame averaging" function and it is convenient to select any number of frames to be averaged. Figure 9b and 9c are images after 6-frame averaging and 20-frame averaging, respectively. Obviously, the image quality is remarkably improved after averaging. And there is no doubt that this approach is very useful especially for insulating polymers when slowing the beam scanning and increasing the scanning resolution are not feasible.

7. Imaging mode selection

The average energy of SEs emitted from the specimen surface is typically 4–5 eV [12]. Such low energy SEs are very vulnerable to charging because their trajectories can be easily altered by local fields. Conversely, BSEs with their higher kinetic energy (up to the incident beam energy) travel in straight lines at high velocities. Therefore the possibility of charging effect at the BSE imaging mode is substantially lower than that at the SE imaging mode. Figure 10a is a SE image showing some charging effects which disappear in the corresponding BSE image, as shown in Figure 10b.

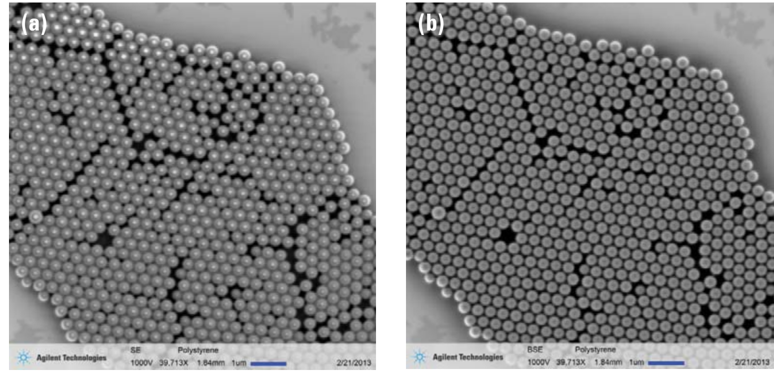

Figure 10. Images of polystyrene beads at different imaging modes: (a) SE; (b) BSE.

In addition to its relatively high immunity to charging, the BSE imaging at low voltages is also very appealing because of its high resolution imaging capability. Since a high voltage electron beam typically produces BSEs emitted from the surface at a distance of up to a few microns from the beam impact area, the BSE imaging mode has a much poorer resolution than the SE one. That is not the case for LV-FESEM where BSEs and SEs have a similar size of interaction volume. Like SEs, BSEs still carry high resolution information because of their emission from the immediate vicinity of the beam incident point. Theoretically, when the beam voltage drops to below 1.5 kV, the depth within the specimen from which BSEs derived information emerges is less than that of SEs and, as a result of this, BSEs can carry more information of surface details [13]. The microchannel plate detector, used in Agilent 8500, is well known for its high sensitivity to slight variations in very low BSE signal intensities [14]. Thus it is not necessary to increase the probe current for a higher BSE emission which may result in a poorer imaging resolution.

8. Effect of angles of the incident beam

It was reported that angles of the incident beam can affect the SE yield δ. When the electron beam impinges the specimen surface at an angle of θ, more interaction volume will move to the surface. Consequently, more SEs are able to escape from the surface leading to a higher SE yield. In a more general form, δ_θ can be expressed as [3, 15]:

$$\delta_\theta = \frac{1}{\cos\theta} \int_0^\infty \frac{f(0)}{\varepsilon} \frac{dE_0}{ds} \exp\left(\frac{-z}{\Lambda}\right) ds \quad (6)$$

where $f(0)$ is a current ratio of SE to incident at the surface, ε is an energy to excite the SE, $(-dE_0/ds)$ is an energy loss per unit length along the incident electron path, Λ is a mean free path of SE, and z is a depth from the surface. Equation **(6)** can be simplified into the following one:

$$\delta_\theta = \frac{\delta_0}{\cos\theta} \quad (7)$$

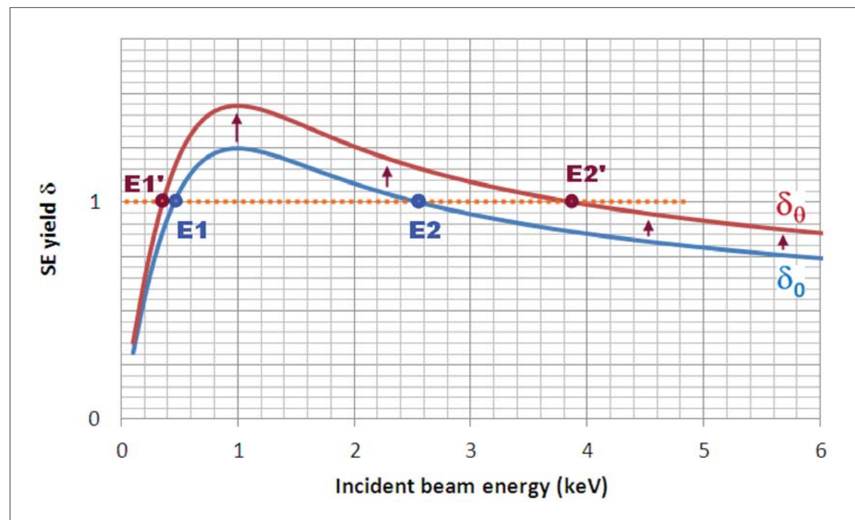

Figure 11. Plot of SE yields at the normal beam incidence (the blue line) and at an angled incidence (the reddish brown line). Note the change of the E_2 value.

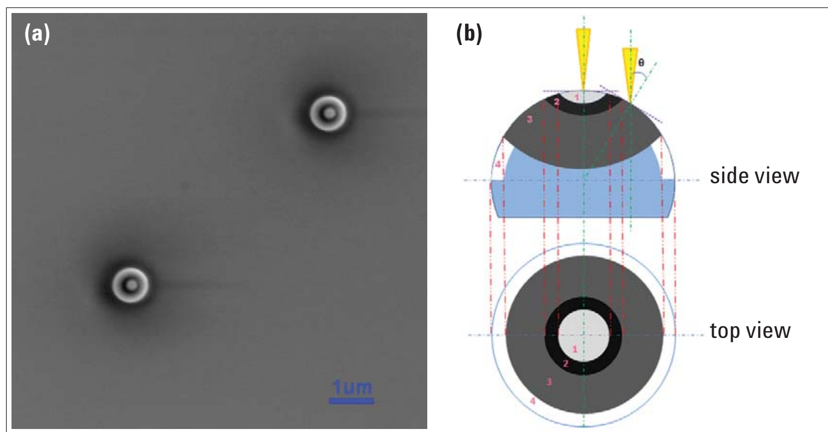

Figure 12. (a) SE image of polystyrene beads at 1 kV with discernable four areas in distinct grey levels showing the charging effect; (b) schematic of the contrast formation due to the incident beam angle and the edge effect.

where δ_0 is the SE yield at a normal angle of incidence. The SE yield curve at an incidence angle is plotted in Figure 11, together with that in the situation of a normal incidence. The figure reveals higher values at all beam voltages for angled beam incidence. Additionally, the E_2 value shifts upwards as the electron beam strikes the specimen in an angle.

According to a model of the charging process, the effective E_2 value with an angled incidence, $E_2(\theta)$, is related with the value at normal incidence $E_2(0)$ as [16]:

$$E_2(\theta) = \frac{E_2(0)}{\cos^2\theta} \qquad (8)$$

Note that equation **(8)** only stands for low-atomic-number materials, such as polymers. This equation implies that, even for the same specimen, areas with different angles respective to the incident electron beam may exhibit different signal intensities. It could be possible that some areas with large angles to the incident beam are positively charged while others with small angles are in the negative charging status. The contrasts shown in Figure 12a as well as Figure 3b can be explained by the incident angle-related SE yield change. Different than Figure 3b, Figure 12a clearly reveals four areas with distinct grey levels on the top surface of each polystyrene sphere. This is possibly due to the less charging and concomitantly less contrast shown in Figure 12a. As illustrated in Figure 12b, area **1** is located around the apex of the sphere where the electron beam impinges the sample roughly in the normal direction. Since the beam energy 1 kV is higher than the estimated value (~700 V) for such a sample, negative potential was developed resulting in a bright area. At area **3**, the beam hits the area in an angle θ due to the curvature of the sphere. According to equation **(8)**, the effective E_2 value changes to $E_2/cos^2\theta$. If an average value is about 45°, the increased E_2 will be ~1.4 kV which is higher than the incident beam energy. Hence, a positive potential was established at this area manifesting itself as a dark area in the image. As discussed in the previous section, area **2** in an even darker color could be caused by the possible local high field retarding the SE detection. The outer most boundary of the sphere, denoted as area **4**, exhibits bright in Figure 12b. In this area, the effect of SEs' depression due to the high incident angle could be overwhelmed by the enhanced edge effect. Thus more SEs can escape because of the high curvature at the edge, and the detected signal on each pixel displays a high intensity. This postulated charging mechanism on polystyrene beads is well consistent with the observation in the whole study throughout: the larger bright area in the center of the sphere with a harsh contrast, the higher magnitude of charging. In an extremely severe charging condition (e.g. E_0>5 keV), the whole polystyrene bead should be in utmost white completely, enabling an impossible feature resolving.

The dependence of the effective E_2 value on the incidence angle actually suggests another effective method to control charging: sample titling, which changes the beam incident angle of the whole specimen overall. Sample tilting is desirable especially when imaging an insulating material has to be carried out at a beam voltage higher than its E_2 value. A noteworthy fact is that the yield increase with beam incident angles becomes less pronounced at low beam voltages. Since most of the beam/specimen interaction volume already falls within the escape range of SEs, sample tilting will not enable many extra

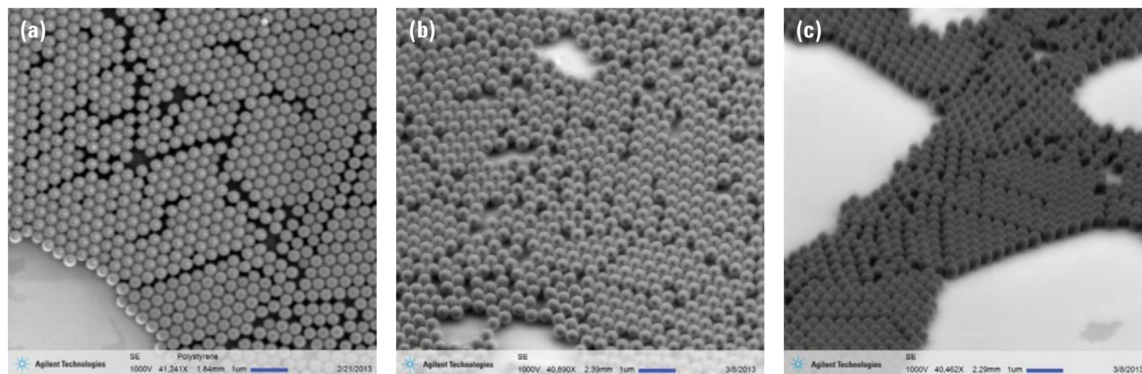

Figure 13. SE images of polystyrene beads at different sample tilt angles: (a) 0°; (b) 30°; and (c) 60°.

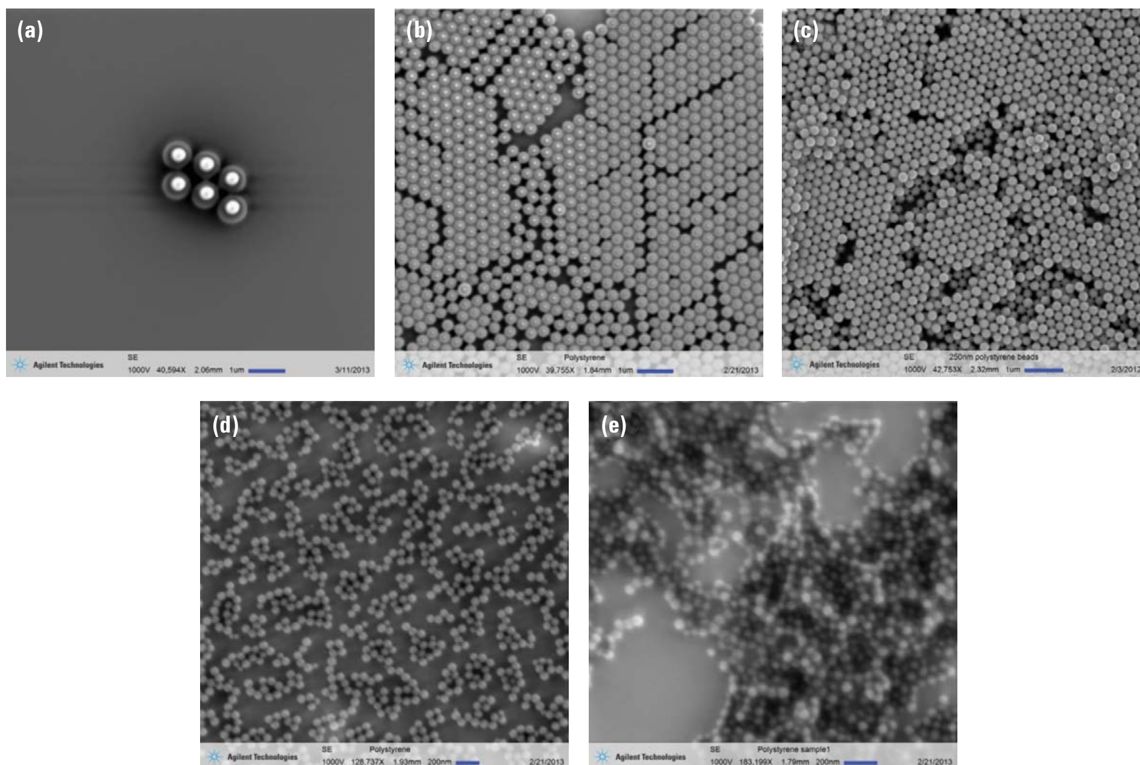

Figure 14. SE images of polystyrene beads with various dimensions: (a) ~850 nm beads; (b) ~400 nm beads; (c) ~250 nm beads; (d) ~100 nm beads; (e) ~50 nm beads. (a–c) were recorded at a similar magnification.

SEs escaping from the surface leading to an enhanced signal. Nevertheless, the increase of SE yields still was observed experimentally at 1 keV despite of its less marked effect than that at higher beam energies (>5 keV) [8].

Tilting the polystyrene beads on a Si substrate was performed in imaging. As shown in Figure 13a, the untilted sample manifests abnormal bright spots on the sphere surface. When the specimen was tilted to 30°, the image Figure 13b, recorded at the identical condition, does not reveal any obvious charging effect. An interesting finding in Figure 13c is that all polystyrene beads exhibits in much darker color at the 60° tilting situation, suggestive of a positive potential establishment on the surface. Considering the sphere geometry of the polystyrene beads, this observation of prominent changes respective to the tilt angle is fairly surprising. It is believed that the horizontal arrangement of polymer spheres and their contact with the Si substrate might contribute the change of SE yield on tilt angles. It is also obvious that the center area in Figure 13c is in focus whereas both the top and bottom areas are out of focus. In LV-FESEM, the working distance, inversely proportional to the depth of field, is normally set to be small in order to minimize the chromatic aberration. Because of this reason, titling samples to high degrees might not be a good option in many situations.

9. Dependence on particle sizes

The effect of particle dimensions on charging is prominent in SEM imaging, as compared in Figure 14(a–c) that were recorded at a similar magnification (~40 kX in the 2048 x 2048 scanning resolution). Polystyrene beads with an average diameter of ~850 nm clearly display an abnormal contrast on account of a negative potential build up on the surface (Figure 14a). Only small bright spots present in Figure 14b for ~400 nm polystyrene beads indicating a much less charging effect at the same condition. For ~250 nm polystyrene beads, charging almost disappears in Figure 14c and the morphological information can be easily obtained from the image. However, charging was observed to emerge when further increased the magnification (>40 kX). Interestingly, it is not difficult at all to image ~100 nm polystyrene beads at much higher magnifications. As shown in Figure 14d, a little bit charging only exists on the upper-right corner when imaging at a magnification of ~120 kX. Following this trend, the charging effect can barely be seen from the image of ~50 nm polystyrene beads recorded at the ~180 kX magnification, as shown in Figure 14e.

The reasons for such a phenomenon described above could be complicated. It was observed that samples with a nanoscale roughness do not charge nearly as quickly as samples with microtextures on a larger scale [4]. Compared with the microscaled structure, the nanoscaled one seems to provide a more favorable geometry for the SE escape from the specimen surface. In the case of polystyrene beads, a smaller sphere possesses a higher curvature. Therefore the less susceptible of smaller beads to charging could be caused by the higher fraction of their top surfaces in tilted angels respective to the electron beam incidence. On the other hand, the properties of materials abruptly change when their dimensions decrease to less than 100 nm. In such a condition,

more atoms are on the surface giving rise to a higher surface area and a higher surface energy. It is believed that the change of physical properties for ~100 nm and ~50 nm polystyrene beads also contributes to their diminutive propensities to the charging effect. Another possible reason could be the improved charge evacuation for nanosized polystyrene beads. According to an empirical formula developed by Kanaya and Okayama, the penetration depth of an incident electron beam R can be calculated as [17]:

$$R = \frac{0.0276 A E_0^{1.67}}{Z^{0.889} \rho} \quad (9)$$

where A is the atomic weight (g/mol), E_0 is the accelerating voltage (keV), Z is the average atomic number and ρ is the density (g/cm^3) of the sample. The penetration depth for primary electrons in polymers is around 70 nm at 1 keV [18]. In the case of ~50 nm beads, when the overall thickness of the specimen is less than the penetration depth, an efficient charge evacuation from the polymer to the conductive support could happen, thus limits the negative potential growth.

Charging Control in Agilent 8500 LV-FESEM

Agilent 8500 is a compact LV-FESEM equipped with a novel miniature all-electrostatic lens system and a microchannel plate detector. Its high performance imaging capability at low voltages is well suitable for morphological characterization of insulating polymeric materials. Based on the effects on charging of polystyrene beads discussed in the previous section, the approaches for charging control that can be implemented on Agilent 8500 is summarized here.

When facing charging phenomena during imaging uncoated polymer specimens, possible approaches can be tried which include: 1) lowering the beam voltage; 2) switching to the BSE imaging mode; 3) reducing the imaging magnification; 4) using a faster scanning rate; 5) selecting a lower scanning resolution, and 6) tilting the specimen. Combination of these approaches might be needed to alleviate the charge accumulation effectively so that a stable image can be recorded in an acceptable quality. General strategies in SEM imaging of insulating polymers always apply. Here are several examples: 1) always ensure a good mounting of polymer specimens with a conducting path to the ground; 2) try to do focusing and astigmation correction as fast as possible to avoid a severe charge accumulation; 3) record the first-scan image at the fresh surface, if possible, for the best image quality; 4) average several frames at a fast scanning rate to reduce the noise. For Agilent 8500, there are a couple of unique features which are beneficial for low voltage imaging of insulating polymers. First, there is no hysteresis effect in the all-electrostatic lens system, and the beam voltage can be adjusted continuously, in the step size of 1V, in the range of 500 V to 2000 V. This extraordinary feature enables a fine tuning of the incident beam's energy for insulating polymers with their E_2 values normally around 1 keV. Secondly, the all-electrostatic lens system offers a unique capability of optimizing imaging parameters in a prompt way. On Agilent 8500, the parameters including column alignment and stigmators can be recorded as a file for future recall. Thus the following operation procedure is quite convenient for imaging non-conductive polymers: 1) conduct focusing, column alignment and astigmation correction at a high magnification on a reduced raster window; 2) after optimization save the condition in a file; 3) navigate to a fresh area and re-focus the feature quickly; 4) recall the pre-saved condition file; 5) record the image immediately. This procedure typically works well especially for highly energy-sensitive materials. Note that the optimized condition is beam voltage dependable and also varies with materials. Therefore, it is necessary to save imaging conditions at certain beam voltages for that particular specimen under investigation.

There is another important machine parameter which is commonly used in traditional SEMs for the charging control purpose yet has not been addressed so far: the probe current. Careful control of the probe current is able to minimize or eliminate the charging problems when working with an incident beam at energy higher than the E_2 of the specimen [8]. The drawback of this approach is that reduction of the probe current normally decreases the signal-to-noise ratio and may lead to an unacceptably high noise level, concomitant with a "grainy" image appearance. The probe current of Agilent 8500 compact LV-FESEM ranges from 200 pA to 1nA. The physical parameters, including the probe current, of the miniature all-electrostatic lens system have been carefully adjusted for an optimized imaging performance at low voltages. Either increasing or reducing the preset probe current in the miniature column may result in a larger spot size and a lower imaging resolution [19]. Thus, despite its capability of charging control, the adjustment of probe current might not be an ideal option on Agilent 8500 LV-FESEM for the purpose of high resolution imaging.

Summary

Without coating, insulating polymeric materials are challenging for SEM imaging. The charging problems, caused by the excess charge accumulation on the specimen surface, are likely to make it difficult to obtain a stable image in high quality. Low voltage field emission SEM is a promising imaging technique for morphological characterization of energy-sensitive polymers, providing effective charging control, enhanced contrasts and high spatial resolutions. Additionally, the low voltage images are expected to be sensitive to the chemical nature and topographic form of the polymer surface. Using sub-micron polystyrene spheres with various dimensions as a paradigm, a number of factors that are related to the charging phenomenon were studied and several strategies were demonstrated towards a charging-free imaging performance in low voltage electron microscopy.

References

[1] D.L. Vezie, E.L. Thomas and W.W. Adams, Polymer 36, 1761 (1995).

[2] G.H. Michler, Electron Microscopy of Polymer, p175, Springer-Verlag Berlin Heidelberg (2008).

[3] A.J. Dekker, Solid State Physics 6, 251 (1958).

[4] J.H. Butler, D.C. Joy, G.F. Bradley and S.J. Krause, Polymer 36, 1781 (1995).

[5] R.F. Willis and D.K. Skinner, Solid State Communications 13, 685 (1973).

[6] E.A. Burke, IEEE Transactions on Nuclear Science NS-27, 1760 (1980).

[7] D.C. Joy, Journal of Microscopy 147, 51 (1987).

[8] D.C. Joy and C.S. Joy, Micron 27, 247 (1996).

[9] Polystyrene samples courtesy of Fudan University and National Institute of Standards and Technologies (NIST).

[10] J. Pawley, Journal of Microscopy 136, 45 (1984).

[11] H. Schatten and J.B. Pawley, Biological Low-Voltage Scanning Electron Microscopy, p64, Springer (2008).

[12] H. Seiler, Journal of Applied Physics 54, R1 (1983).

[13] R.G. Richards, G.Rh. Owen and I. ap Gwynn, Scanning Microscopy 13, 55 (1999).

[14] M.T. Postek, W.J. Keery and N. Frederick, Review of Scientific Instruments 61, 1648 (1990).

[15] T. Ichinokawa, M. Iiyama, A. Onoguchi and T. Kobayashi, Japanese Journal of Applied Physics 13, 1272 (1974).

[16] D.C. Joy, Scanning 11, 1 (1989).

[17] K. Kanaya and S.J. Okayama, Journal of Physics D: Applied physics 5, 43 (1972).

[18] C. Gaillard, P.A. Stadelmann, C.J.G. Plummer and G. Fuchs, Scanning 26, 122 (2004).

[19] J.P. Spallas, C.S. Silver and L.P. Muray, Journal of Vacuum Science and Technologies B 24, 2892 (2006).

Nanomeasurement Systems from Agilent Technologies

Agilent Technologies, the premier measurement company, offers high-precision, modular nanomeasurement solutions for research, industry, and education. Exceptional worldwide support is provided by experienced application scientists and technical service personnel. Agilent's leading-edge R&D laboratories ensure the continued, timely introduction and optimization of innovative, easy-to-use nanomeasure system technologies.

www.agilent.com/find/nano

Americas

Canada	(877) 894 4414
Latin America	305 269 7500
United States	(800) 829 4444

Asia Pacific

Australia	1 800 629 485
China	800 810 0189
Hong Kong	800 938 693
India	1 800 112 929
Japan	0120 (421) 345
Korea	080 769 0800
Malaysia	1 800 888 848
Singapore	1 800 375 8100
Taiwan	0800 047 866
Thailand	1 800 226 008

Europe & Middle East

Austria	43 (0) 1 360 277 1571
Belgium	32 (0) 2 404 93 40
Denmark	45 70 13 15 15
Finland	358 (0) 10 855 2100
France	0825 010 700* *0.125 € /minute
Germany	49 (0) 7031 464 6333
Ireland	1890 924 204
Israel	972-3-9288-504/544
Italy	39 02 92 60 8484
Netherlands	31 (0) 20 547 2111
Spain	34 (91) 631 3300
Sweden	0200-88 22 55
Switzerland	0800 80 53 53
United Kingdom	44 (0) 118 9276201

Other European Countries:
www.agilent.com/find/contactus

Product specifications and descriptions in this document subject to change without notice.

© Agilent Technologies, Inc. 2013

Printed in USA, May 3, 2013
5991-2414EN

Agilent Technologies